Quantum calculations of nonadiabatic $^2A_1$–$^2B_2$ conical-intersection effects in the reactions N(^4S) + O$_2$($X^3\Sigma_g^-$) and N(^4S) + O$_2$($A^3\Delta_u$)

Paolo Defazio [a], Sinan Akpinar [b], Carlo Petrongolo [a,c,*]

[a] *Dipartimento di Chimica, Università di Siena, Via A. Moro 2, I-53100 Siena, Italy*
[b] *Department of Physics, Firat University, 23169 Elazig, Turkey*
[c] *Istituto per i Processi Chimico-Fisici del CNR, Via G. Moruzzi 1, I-56100 Pisa, Italy*

ABSTRACT

We present both the Born–Oppenheimer (BO) and the nonadiabatic (NA) conical-intersection quantum dynamics of the title reactions, (1) and (2), respectively. BO or NA calculations are carried out using adiabatic or diabatic electronic states, respectively, and we consider some vibrational (v_0) and rotational (j_0) states of O$_2$, taking into account the Pauli principle. The results reflect the barrier or barrierless nature of reaction (1) or (2), respectively, and the former is, thus, much less reactive than the latter. Reaction (1) is direct and its probabilities and cross sections increase with the collision energy from a threshold value, are slightly affected by NA couplings only at high energies, increase with v_0, and are essentially unchanged by j_0. On the contrary, reaction (2) is indirect and its probabilities and cross sections decrease with the collision energy without any threshold, are significantly lowered by NA couplings at low energies, and decrease with both v_0 and j_0.
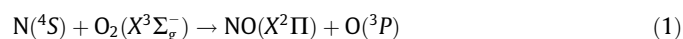
© 2010 Elsevier B.V. All rights reserved.

1. Introduction

The NO$_2$ molecule plays a central role in many combustion, atmospheric, astrochemical, and plasma elementary processes, and its spectroscopic and dynamical properties were deeply investigated from many years. NO$_2$ presents a very anomalous, complex, and irregular spectrum, which resisted a detailed understanding up to 1975 and 1976, when the theoretical works by Gillispie et al. [1] and Jackels and Davidson [2] reported a C_{2v} $^2A_1$–$^2B_2$ conical intersection (CI) between the ground $\tilde{X}^2A'$ and first excited $\tilde{A}^2A'$ adiabatic electronic states. We call these states $\tilde{X}$ and $\tilde{A}$, with potential energy surfaces (PESs) V_X and V_A, respectively. Subsequently, Köppel et al. [3] were the first to go beyond the Born–Oppenheimer (BO) approximation and to present a nonadiabatic (NA) theoretical work, based on two diabatic electronic states coupled by a simple electronic potential, for qualitatively reproducing the experimental absorption spectrum. Since the first detailed experimental work by Delon and Jost [4], who strongly improved on previous experiments, it was shown that this CI has a huge impact on levels and states, on absorption spectra, on energy- and time-resolved fluorescence spectra, and on the photo-induced internal dynamics [5]. Boltzmann partition functions and thermodynamical observables are also remarkably affected by this CI [6].
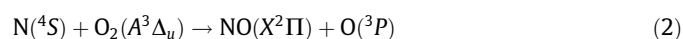
The NO$_2$ $\tilde{X}$ and $\tilde{A}$ states are also involved in N + O$_2$ and NO + O reactions, and their $^2A_1$–$^2B_2$ CI can thus be important also in collision dynamics. For example, the lowest six electronic states of the reactants N(^4S, ^2D, or ^2P) + O$_2$($X^3\Sigma_g^-$, $a^1\Delta_g$, $b^1\Sigma_g^+$, or $A^3\Delta_u$), up to 4.30 eV above N(^4S) + O$_2$($X^3\Sigma_g^-$), correlate to six $^2A_1$ and seven $^2B_2$ electronic states of NO$_2$, which can give many CIs and avoided crossings. We plot in Fig. 1 a schematic correlation diagram, based on the theoretical work of Varandas and Voronin [7,8], showing only the ground and the fifth-excited N + O$_2$ channels, i.e. the reactions

$$N(^4S) + O_2(X^3\Sigma_g^-) \rightarrow NO(X^2\Pi) + O(^3P) \qquad (1)$$

and

$$N(^4S) + O_2(A^3\Delta_u) \rightarrow NO(X^2\Pi) + O(^3P) \qquad (2)$$

Reaction (1) was investigated by many authors, who showed that it proceeds mainly via NO$_2$($\tilde{X}$) up to about 2000 K, where the $\tilde{X}^2A'$ C_{2v} symmetry is $^2B_2$ or $^2A_1$ before or after the CI, respectively. For example, product distributions were measured at room temperature [9] and at a collision energy of about 3 eV [10], and the experimental rate constant is known from 298 to 5000 K [11]. The most recent calculations of V_X were performed in [8,12,13]. In particular, Varandas [8] reported the lowest eight $^2A'$ PESs, Sayós et al. [12] presented the V_X and $1^4A''$ PESs, and Kurkal et al. [13] calculated the V_X and V_A PESs and an associated diabatic representation. With respect to the N(^4S) + O$_2$($X^3\Sigma_g^-$) reactants, the V_X surface of [8] has C_s and C_{2v} barriers at 0.27 and 1.08 eV,
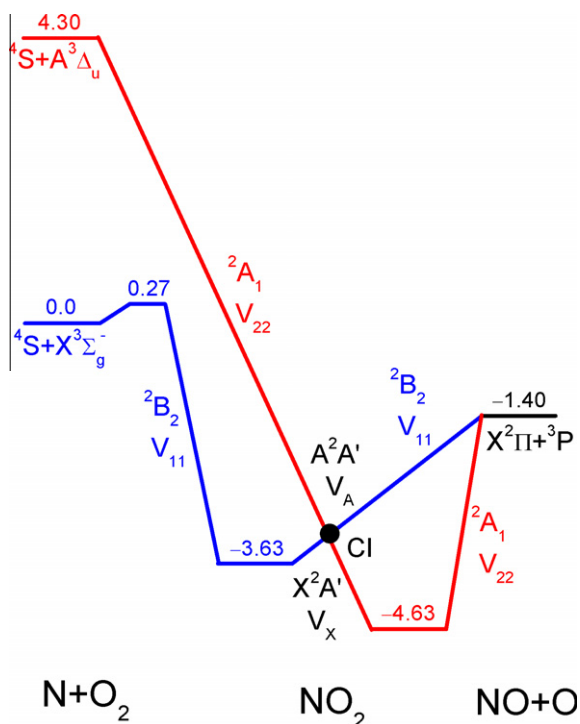
Fig. 1. Schematic correlation diagram of the NO$_2$ $\tilde{X}^2A'$ and $\tilde{A}^2A'$ electronic states, involved in reactions (1) and (2) [7,8]. Energies in eV with respect to N(^4S) + O$_2$($X^3\Sigma_g^-$, r_{eq}).

respectively, and two C_{2v} minima, $^2B_2$ at -3.63 eV and $^2A_1$ at -4.63 eV. These minima are due to the CI and are separated by a C_{2v} intersection locus whose minimum energy is equal to -3.42 eV. Finally, reaction (1) is exoergic by 1.40 eV. Theoretical dynamical studies of this collision were also performed. For example, product distributions and rate constants were calculated in [14], and reaction probabilities, cross sections, rate constants, and product distributions were presented in [15].

As far as we know, reaction (2) was never investigated previously. The N(^4S) + O$_2$($A^3\Delta_u$) reactants are 4.30 eV above those of reaction (1), and correlate adiabatically with NO$_2$($\tilde{A}$) whose C_{2v} symmetry is $^2A_1$ or $^2B_2$ before or after the CI, respectively. According to [8], the associated V_A PES does not present any barrier.

All past calculations of the N + O$_2$ reaction dynamics were carried out within the BO approximation, without taking into account the $^2A_1$–$^2B_2$ CI. Because NA effects are very important in the NO$_2$ spectroscopy, here we present a quantum-mechanical study of the dynamics of the reactions (1) and (2), considering the CI couplings between the $\tilde{X}$ and $\tilde{A}$ states of NO$_2$. We use the Varandas [8] V_X and V_A PESs, which were obtained via a multi-sheeted double many-body expansion method. Because V_X spectroscopic accuracy was reached via a multiple energy-switching scheme, these PESs are the best available for describing the $^2A_1$–$^2B_2$ CI. Owing to the high C_{2v} barrier, reaction (1) should proceed adiabatically on the V_X surface, at low and intermediate collision energies, along the C_s minimum energy path (MEP). However, reaction (2) is barrierless and we thus expect that it presents remarkable NA effects, associated with the C_{2v} $^2A_1$–$^2B_2$ CI.

The quantum investigation of the CI dynamics in the adiabatic representation is however very complicated, because it requires the knowledge of nine 3D surfaces of the first- and second-derivative vibronic couplings, some of which were calculated at a few geometries many years ago [16]. Therefore, we here employ a diabatic representation that minimizes the vibronic couplings and relies on the adiabatic Varandas PESs V_X and V_A [8] and on the

diabatic electronic coupling V_{12} of Leonardi et al. [17]. In particular, we obtain the diabatic PESs V_{11} and V_{22} from V_X, V_A, and V_{12} via standard formulas, and we perform the quantum dynamics on the three diabatic surfaces $V_{e'e}$.

2. Theory and calculations

As in our previous works on $X + Y_2$ collisions [18], we employ the permutation-inversion group $C_{2v}(M)$ and the reactant Jacobi coordinates R, r, and γ, and we represent the spinless molecular states $|nJMp\rangle$ on an electronic, vibrational, and rotational basis $|e\rangle \times (|Rr\rangle \times |jK\rangle) \times |K\sigma p\rangle$. Here J and M are the total angular momentum quantum number and its projection along a space fixed axis, respectively, $p = \pm$ is the total parity, $|e\rangle$ and $|Rr\rangle$ are electronic and radial states, respectively, $|jK\rangle$ are associated Legendre states, where $K \geqslant 0$ is the projection of J along **R**, and $|K\sigma p\rangle$ are symmetry-adapted Wigner states, where $\sigma = \pm$ is the electronic parity. For $|e\rangle \sim A_1$ or B_2 and $j =$ even or odd, Table 1 reports the symmetries of the $|n\rangle$ states; for $|e\rangle \sim A_2$ or B_1, the $|n\rangle$ symmetries associated with $|e\rangle \sim A_1$ must be multiplied by A_2 or B_1, respectively. Because the ^{16}O nuclear spin is equal to 0, the Pauli principle implies that the ^{14}N^{16}O$_2$ $|n\rangle$ states must be symmetric under the permutation of the ^{16}O nuclei, i.e. of A_1 or A_2 symmetry. Therefore, j must be odd for reaction (1), N(^4S) + O$_2$($X^3\Sigma_g^-$) → NO$_2$($^2B_2$), and even for reaction (2), N(^4S) + O$_2$($A^3\Delta_u$) → NO$_2$($^2A_1$), and these j values are coupled by the $^2A_1$–$^2B_2$ CI.

From the equations

$$V_X = \frac{1}{2}\left[V_{11} + V_{22} - \sqrt{(V_{11} - V_{22})^2 + 4V_{12}^2}\right],$$

$$V_A = \frac{1}{2}\left[V_{11} + V_{22} + \sqrt{(V_{11} - V_{22})^2 + 4V_{12}^2}\right], \tag{3}$$

we obtain the following expressions of the diabatic surfaces

$$V_{11} = \frac{1}{2}\left[V_X + V_A \pm \sqrt{(V_X - V_A)^2 - 4V_{12}^2}\right],$$

$$V_{22} = \frac{1}{2}\left[V_X + V_A \mp \sqrt{(V_X - V_A)^2 - 4V_{12}^2}\right]. \tag{4}$$

The ambiguities of the plus or minus signs in (4) are removed by computing and fitting the CI locus at $\gamma = 90°$ as

$$R_{CI}(r) = 11.73561 - 29.7791r + 26.804r^2 - 10.68286r^3$$
$$+ 1.97305r^4 - 0.13821r^5, \tag{5}$$
$$1.3230 \leqslant r \leqslant 4.8263,$$

where we use a.u. We plot this locus in Fig. 2 together with two PES regions, (I) and (II), where we take the plus and minus sign in V_{11} and V_{22}, respectively, if $R \leqslant R_{CI}(r)$ and vice versa if $R > R_{CI}(r)$. Therefore, Fig. 2 shows that V_{11} correlates with N(^4S) + O$_2$($X^3\Sigma_g^-$) and NO$_2$($^2B_2$), and V_{22} correlates with N(^4S) + O$_2$($A^3\Delta_u$) and NO$_2$($^2A_1$). In C_{2v}, $V_{11} = V_X$ or V_A before or after the CI, respectively, and the opposite holds for V_{22}.

In [17], the NO$_2$ coupling V_{12} was optimized with respect to the observed vibronic bands up to 1.47 eV above the $\tilde{X}^2A'$ potential well [4], which lies at -4.63 eV below the N(^4S) + O$_2$($X^3\Sigma_g^-$) reactants [8]. In particular, the long-range V_{12} was empirically damped

Table 1
$C_{2v}(M)$ symmetry of spinless molecular states $|n\rangle$.

$|e\rangle$	j	$|n\rangle$
A_1	Even	A_1 or A_2
	Odd	B_1 or B_2
B_2	Even	B_1 or B_2
	Odd	A_1 or A_2